Geol. Mag. **142** (2), 2005, pp. 145–158. © 2005 Cambridge University Press
doi:10.1017/S001675680400041X *Printed in the United Kingdom*

Petrology and potential tectonic significance of a K-bentonite in a Taconian shale basin (eastern Ontario, Canada), northern Appalachians

SAJAL SHARMA*‡, GEORGE R. DIX* & MIKE VILLENEUVE†

*Ottawa-Carleton Geoscience Centre and Department of Earth Sciences, Carleton University, 1125 Colonel By Drive, Ottawa, ON K1S 5B6, Canada
†Geological Survey of Canada, 601 Booth Street, Ottawa, ON K1A OE8, Canada

(*Received* 3 June 2004; *accepted* 8 November 2004)

Abstract – A 6 cm thick K-bentonite, herein defined as the Russell Bed, occurs in an Upper Ordovician deep-basin shale succession in eastern Ontario, Canada, forming part of the distal Taconic foreland in eastern North America. The bed lies within the *pygmaeus* graptolite Biozone, which is about 451 to 452 Ma in age. Although some bentonites are reported from this interval in eastern North America, we are reporting the first set of compositional data for a bentonite of this age. Gamma-log correlation identifies a potential minimum distribution area of $< 2 \times 10^5$ km^2 for the K-bentonite, covering part of southern Quebec, New York State and eastern Ontario. The deposit coincides with the first influx of distal turbdites into this shale basin, associated with Taconic flysch, and simultaneous abrupt ventilation of the once anoxic deep-water basin, which had formed initially after foundering of the Upper Ordovician carbonate platform. Concurrent intrabasinal extinction of several graptolite species suggests that change in sedimentation, palaeoceanography and volcanism were linked to a regional external process. Compositionally, the bentonite is distinct from the older Ordovician platform deposits in eastern North America. The deposit contains abundant titaniferous phlogopite with 1.6% BaO, fluoroapatite with 2.5% F, and dynamically shaped glass spherules now altered to clay. The spherules and clay matrix constitute 45% of the bed and, compositionally, define an illite (> 90%)–smectite (I/S) structure with about 7.5% K_2O%. Age-dating by Ar–Ar analysis of the phlogopite crystals yielded a younger than expected (440–445 Ma) age. This difference, along with evidence of localized chloritization of phlogopite, likely reflects known post-Ordovician hydrothermal activity within the basin. On the basis of several geochemical proxies, the magmatic source of the Russell K-bentonite falls within the trachyandesite field and was Ba-enriched. Comparison of geochemistry and mineralogy with older, Middle to Late Ordovician and younger Early Silurian K-bentonites within the Taconic orogen along eastern Laurentia and Baltica reveals that the potential source magma for the Russell Bed was more mafic, more alkaline, and less fractionated than sources typical of older (platform) bentonites. Instead, it is more similar to the younger Llandovery bentonites of Scandinavia and Scotland. It remains uncertain if it signals local or regional compositional change in volcanic source in the northern Appalachians.

Keywords: K-bentonite, Ontario, Upper Ordovician, flysch, shale.

1. Introduction

Numerous K-bentonites occur within the Middle Ordovician to Silurian sedimentary succession of eastern Laurentia and Baltica, now preserved in eastern North America, the UK and Scandinavia (Fig. 1a, b). Within the Middle to Upper Ordovician carbonate platform succession (the Trenton Group) of the Taconic foreland basin in eastern North America, the Millbrig, Deicke and Kinnekulle deposits (Fig. 1a) are the best known and studied; they represent volcanic ash beds deposited in shallow water and derived largely from rhyolitic to rhyodacitic sources (Samson, Kyle & Alexander, 1988; Delano *et al.* 1994; Haynes, 1994; Bergström & Mitchell, 1994; Kolata, Huff & Bergström, 1996; Min, Renne & Huff, 2001). Along the same orogenic belt, but in southern Scotland and Scandinavia (Fig. 1a), Middle to Upper Ordovician K-bentonites also identify rhyolitic to rhyodacitic sources (Batchelor & Weir, 1988; Merriman & Roberts, 1990; Batchelor, 2003). However, some younger Silurian (Llandovery) bentonites exposed in Scotland and Scandinavia demonstrate that a prominent change in magmatic composition had occurred, yielding intermediate alkaline sources (Batchelor & Jeppson, 1994).

In eastern Ontario, Canada (Fig. 2), an Upper Ordovician (451–452 Ma) deep-water shale succession contains a newly discovered K-bentonite (S. Sharma, unpub. Ph.D. thesis, Carleton Univ., Canada, 2004).

‡ Author for correspondence: sajalsharma@sprint.ca

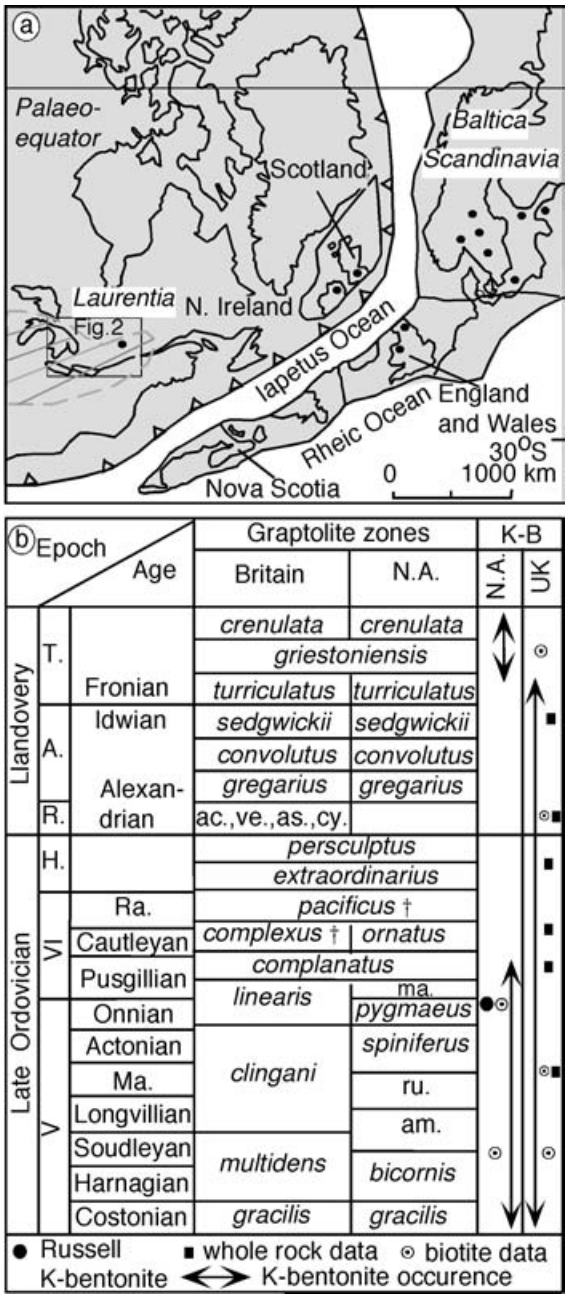

Figure 1. (a) Palaeogeographic map of Laurentia and Baltica during Llandloverian time (after McKerrow, Dewey & Scotese, 1991) illustrating study location (box outline) and general locations of other K-bentonites referred to in the text. Filled circle, locations of Late Ordovician and Silurian K-bentonites; hatched area, location of Deicke and Millbrig K-bentonite in eastern USA. (b) Stratigraphic position of the Russell K-bentonite with respect to other Late Ordovician and Early Silurian K-bentonites (K-B) from eastern North America (N.A.) and the United Kingdom (UK). International Stratigraphic Chart by International Commission on Stratigraphy, 2004 is followed. Epoch and Age abbreviations: T. – Telychian; A. – Aeronian; R. – Rhuddanian; H. – Hirnantian; Ra. – Rawtheyan; Ma. – Marshbrookian. Graptolite zonations are from Bergström *et al.* (1997), Woodcock (2000) and Webby *et al.* (2004). † – *complexus* and *pacificus* zones comprise the *anceps* Zone in Britain. Abbreviated graptolite zones from oldest to youngest: am. – *americanus*; ru. – *ruedemanni*; ma. – *manitoulinensis*; ac. – *acuminatus*; ve. – *vesiculosus*; as. – *acinaces*; cy. – *cyphus.*

Compared to the well-studied older Ordovician carbonate platform-hosted bentonites, volcanic-derived deposits in the overlying deep-water Ordovician shales (*pygmaeus* to *persculptus* graptolite zones) are poorly known and preserved, and, of those documented, no mineralogical or geochemical data have been reported (Baird & Brett, 2002). The petrological characteristics of the K-bentonite in Ontario defines an intermediate, alkaline magmatic source more similar to the Early Silurian Scottish and Scandinavian occurrences than to the older platform-hosted deposits of eastern North America. Furthermore, volcanism coincided with prominent changes in local basin development, following collapse of the carbonate platform in this foreland basin. While the regionality of this compositional contrast awaits future study of other basin-hosted Late Ordovician bentonites in eastern North America, the stratigraphic position of the K-bentonite in Ontario may illustrate the change in volcanic source composition during the Late Ordovician allied with basin tectonism.

2. Stratigraphic framework

Along the length of the Taconic orogen in eastern North America, an Upper Ordovician carbonate platform succession (the Trenton Group, and its equivalent) is succeeded by local deep-water shale basins (Diecchio, 1991). In eastern Ontario, Canada, the platform-to-basin succession is recorded by the Lindsay and Billings formations (Fig. 3; Sanford, 1993), with the basin succession containing sediment distal to the developing magmatic Taconic arcs. The local basin was filled rapidly by westward-transported flysch, culminating in accumulation of the peritidal Queenston Formation (Sharma & Dix, 2004). Only a small geographic region in eastern Ontario is now underlain by the deep basin succession, due to post-Ordovician erosion (Fig. 2).

The Billings Formation contains a lower clayshale that records anoxic to dysaerobic deep-water conditions, and an upper clayshale with interbedded siltstone and fine-grained sandstone that represents influx of distal turbidity flows (Fig. 3; Sharma, Dix & Riva, 2003). The appearance of these flows coincided with abrupt deep-water ventilation and the basin-wide extinction of four graptolite species (Sharma, Dix & Riva, 2003).

The K-bentonite described herein, and designated as the 'Russell Bed', was discovered in core in the GSC (Geological Survey of Canada) Russell No. 2 well, Russell County (Fig. 2). The bed occurs at the lower–upper unit boundary of the Billings Formation, 12 m above the top of the carbonate platform. The K-bentonite occurs within the *Geniculograptus pygmaeus* graptolite Biozone (Fig. 1b; Sharma, Dix & Riva, 2003), ~451–2 Ma in age (Webby *et al.* 2004).

https://doi.org/10.1017/S001675680400041X Published online by Cambridge University Press

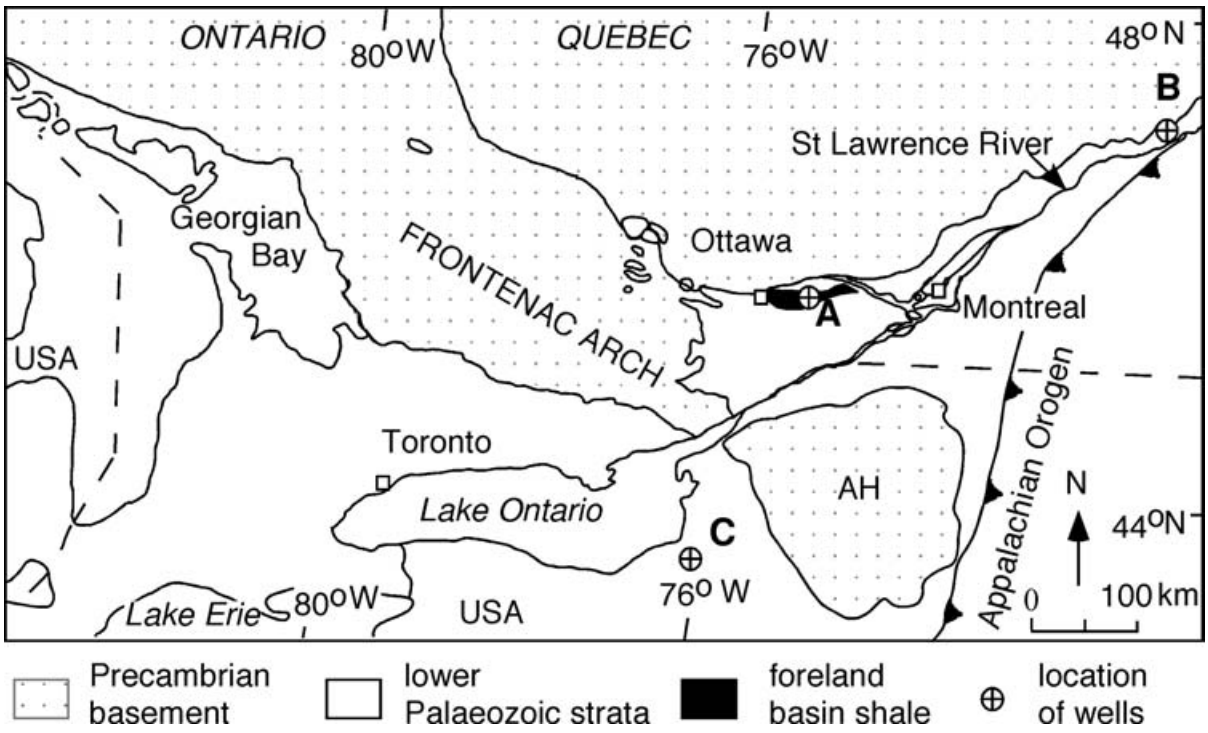

Figure 2. Regional bedrock geology of southern Ontario (inset in Fig. 1a) showing general distribution of lower Palaeozoic and Precambrian rocks (modified from Sanford, 1993). The Russell Bed was discovered at Loc. A (UTM: 469400 mE, 5017600 mN, zone 18, NAD 1927). Sites containing possible time-equivalent deposits are indicated: B – Verchers well, southern Quebec, and C – House well, New York State (NYS), both cited by Bergström & Mitchell (1994). AH – Adirondack Highlands.

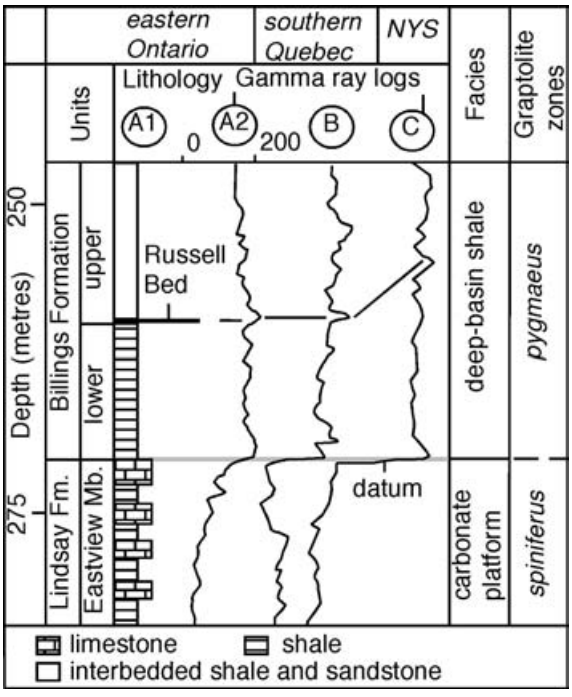

Figure 3. Lithology and graptolite biostratigraphy for Loc. A drill core (A1) is shown relative to general carbonate-shale division of the foreland succession in eastern Ontario. Gamma ray logs and possible regional correlation are shown for Locs A2, B, C (Bergström & Mitchell, 1994; Kolata, Huff & Bergström, 1996; Sharma, Dix & Riva, 2003). Well A2 (UTM: 468295 mE, 5012899 mN) is adjacent to Loc. A1, and the well log is shown in API units. API units are not available for other localities.

3. Methods

The Russell core is 4 cm in diameter, one half preserved at Ottawa, GSC, Tunney's Pasture. Samples for polished thin-sections or for disaggregation were taken at the base, middle and top of the K-bentonite bed. Gamma-ray wireline logs were used to establish possible regional subsurface correlation. Constituent percentages were determined by point counting (n = 300). Whole rock samples were gently crushed and disaggregated in water to remove framework grains. These were examined using scanning electron microscopy (SEM). X-ray, CuKα diffractometry (XRD) at Carleton University was used to analyse unoriented powder for bulk rock, and oriented mount with/without glycol solvation for clay mineralogy following Moore & Reynolds (1997). Whole rock geochemistry for major and selected trace elements, and rare earth elements (Table 1) was determined by X-ray fluorescence and inductively coupled plasma mass spectrometry at the Ontario Geological Survey, Sudbury. A CAMEBAX microprobe at Carleton University, with settings of 17 kV, 10–20 s counting times, 100 ppm detection limit, and 1–3% relative error, provided spot-analysis for major and selected trace elements (Table 2). Raw data were converted to elemental weight% using Cameca's PAP matrix program. The MINPET program was used to recalculate biotite mineral formulae and the $Mg/(Mg + Fe^{2+})$ ratio. A ratio of 3:1 for FeO and Fe_2O_3 was assumed where only total FeO was

https://doi.org/10.1017/S001675680400041X Published online by Cambridge University Press

Table 1. Geochemistry of Russell Bed and Ordovician K-bentonites

	A* (n = 1)	B (n = 4)	C (n = 1)	D (n = 1)	E (n = 17)	F (n = 128)
SiO_2	40.72	62.50	50.17	56.83	58.74	N.A.§
	49.05	[0.73]			[0.67]	
TiO_2	0.90	0.78	1.95	0.98	0.40	0.40
	1.00	[0.02]			[0.05]	[0.02]
Al_2O_3	27.56	16.38	28.24	29.04	22.52	N.A.
	29.76	[0.43]			[0.56]	
FeO	21.25#	6.55#	7.83	2.54	1.65#	2.08#
	8.40#	[0.22]			[0.15]	[0.11]
MnO	0.03	0.07	0.07	0.22	0.01	N.A.
	0.03	[0.00]			[0.00]	
MgO	2.84	2.82	2.44	2.57	4.12	N.A.
	2.84	[0.12]			[0.09]	
CaO	0.28	2.20	0.68	0.57	2.90	N.A.
	0.28	[0.24]			[0.75]	
Na_2O	0.55	1.13	0.27	0.27	0.65	0.05
	0.55	[0.07]			[0.07]	[0.00]
K_2O	6.13	3.89	8.13	6.91	7.67	9.39
	6.65	[0.18]			[0.19]	[0.21]
BaO	N.A.	N.A.	N.A.	N.A.	N.A.	N.A.
P_2O_5	0.15	0.19	0.25	0.05	0.08	N.A.
	0.21	[0.02]			[0.01]	
Total	100.41	96.52	100	100	100.91	N.A.
La	6.62		58.4	75.5		
Ce	14.22		219	208		
Pr	1.60		N.A.	N.A.		
Nd	6.08		113	87		
Sm	1.11		20.5	14.7		
Eu	0.30		5	3.71		
Gd	1.04		N.A.	N.A.		
Tb	0.17		1.58	1.47		
Dy	1.38		N.A.	N.A.		
Ho	0.35		N.A.	N.A.		
Er	1.07		N.A.	N.A.		
Tm	0.19		N.A.	N.A.		
Yb	1.26		4.45	4.22		
Lu	0.20		0.59	0.54		
Nb	10.6		49	43		
Y	10.27		65	63		
Zr	318.27		517	757		
Pb	38.8		N.A.	N.A.		
U	10		2.62	0.89		
Th	9.05		26.3	35.3		

Numbers in brackets indicate standard errors. *A, B – Russell K-bentonite and enveloping shale, respectively; C, D – Ordovician K-bentonites from southern Scotland (Merriman & Roberts, 1990); E, F – Ordovician K-bentonites Trevail (1990) and Kolata, Frost & Huff (1986); respectively. § N.A. = not available; # Fe_2O_3.

reported (Haynes, Melson & Kunk, 1995). Laser $^{40}Ar/^{39}Ar$ analysis (see Appendix 1) of selected biotite phenocrysts was carried out at the Geological Survey of Canada, Ottawa.

4. The Russell K-bentonite bed

4.a. Occurrence and distribution

The bed is 6 cm thick, dark grey and massive. It is set apart macroscopically from surrounding shales by conspicuous large, < 500 μm, euhedral phlogopite crystals. Gamma ray wireline logs from wells within ~ 5 km of the Russell well illustrate a relatively strong positive gamma ray deflection at this stratigraphic level (Fig. 3). Similar deflections in shales at approximately the same stratigraphic position above the top of the Trenton carbonate platform at other sites in Quebec and New York (Fig. 3) may identify a similar occurrence. North of Montreal, about 150 km east of the Russell well, Clark & Stevenson (1960) reported euhedral micas, stated to be biotite, in outcrop. The abundance of these micas decreases over metres moving up-section from the top of the Trenton carbonate platform. As there is no other information on local lithology, regional variation in sedimentation rates or biostratigraphy, it remains uncertain if the individual gamma ray deflections and outcrop occurrence are part of a regional bed or discrete units closely distributed in time.

4.b. Fabric, texture and constituents

The lower boundary of the Russell K-bentonite is abrupt. Thin-section analysis reveals an apparent fining-upward succession of constituent apatite and phlogopite crystals in the lower few millimetres of the bed. There are discontinuously infolded microlaminae within the bed that may identify soft-sediment deformation. The upper boundary of the bed is gradational. There is an increased abundance of siliciclastic detritus in the uppermost 5 mm of the bed, and minor amounts of reworked euhedral, lath-shaped constituent crystals.

Texturally, the Russell Bed is bimodal. About 45% of it is clay matrix that supports phenocrysts (90%), clay spherules (7%) and rounded mudrock lithic fragments (3%) (Fig. 4a). Of the phenocrysts, euhedral phlogopite and fluoroapatite represent < 62 and < 11%, respectively, and range in size from 100 to 500 μm (Fig. 4b). Of the fluoroapatite, a subset of crystals is lath shaped, 5–10 μm in size. Fluorapatite occurs rarely as solid inclusions in phlogophite crystals, and some phlogophite crystals possess a thin (2 to 4 μm) rim of clay similar in texture to, but disconformably demarcated from, the surrounding clay matrix (Fig. 4a). Some apatite crystals also contain glass inclusions. Accessory phenocrysts include untwinned albite of < 8%, magnetite < 4% and zircon in trace, as well as replacement pyrite of < 12% and chalcopyrite in trace. Clay spherules, 50–150 μm in size are spherical, teardrop and elongate in shape, and possess variably smooth to finely and irregularly pitted surfaces (Fig. 4a, c). In thin-section under plain light, they exhibit yellow, orange and light brown colours. Compactional effects are visible in thin-section (Fig. 4a).

4.c. Mineralogy and geochemistry

Bulk rock XRD confirms petrographic observations that phlogopite, apatite, albite and pyrite are principal constituents. Quartz is absent in sharp contrast to its relative abundance in the bounding shales. Microprobe

https://doi.org/10.1017/S001675680400041X Published online by Cambridge University Press

Table 2. Geochemistry of volcanic fragments

	Micas			Volcanic glass			
	A† (n = 13)	B (n = 7)	C (n = 8)	A (n = 3)	D (n = 20)	E (n = 1)	F (n = 20)
SiO_2	36.99 [0.07]	35.54 [0.26]	36.06 [0.32]	49.85 [0.42]	46.48 [0.04]	50.90	50.36 [0.07]
TiO_2	5.47 [0.06]	4.30 [0.14]	4.75 [0.1]	0.06 [0.04]	4.51 [0.02]	0.29	2.29 [0.01]
Al_2O_3	14.17 [0.1]	14.57 [0.44]	13.48 [0.1]	33.69 [0.45]	12.58 [0.03]	24.47	13.93 [0.02]
FeO	12.33 [0.2]	21.23 [0.7]	19.16 [0.72]	2.28 [0.78]	14.55 [0.04]	0.62	12.75 [0.08]
MnO	0.18 [0.02]	0.14 [0.02]	0.18 [0.02]	0.01 [0.01]	0.20 [0.02]	0.02	N.A.
MgO	15.84 [0.12]	9.86 [0.60]	11.51 [0.42]	1.95 [0.3]	4.98 [0.07]	3.65	6.01 [0.03]
CaO	0.01 [0.00]	0.06 [0.01]	0.04 [0.01]	0.08 [0.05]	9.62 [0.19]	0.50	10.08 [0.03]
Na_2O	0.61 [0.02]	0.49 [0.03]	0.37 [0.01]	0.16 [0.02]	3.03 [0.06]	1.07	2.80
K_2O	8.26 [0.05]	8.89 [0.07]	8.87 [0.1]	7.68 [0.89]	0.74 [0.04]	7.26	0.56 [0.01]
BaO	1.64 [0.06]	0.41 [0.09]	0.45 [0.07]	0.14 [0.13]	N.A.	N.A.	N.A.
Cl	0.03 [0.00]	0.11 [0.01]	0.14 [0.03]	0.19 [0.18]	N.A.	N.A.	N.A.
F	0.96 [0.02]	0.76 [0.07]	0.59 [0.06]	0.32 [0.21]	N.A.	N.A.	N.A.
Total	96.50	96.38	95.61	96.41	96.70	99.56	98.98

A – Russell K-bentonite; B, C – Millbrig and Deicke (Min, Renne & Huff, 2001); D – Basaltic Vedde ash shards, Late Quaternary (Davies, Turney & Lowe, 2001); E – I/S altered from Ordovician volcanic glass (Huff & Türkmenoglu, 1981); F – glass spherules (Melson, O'Hearn & Fredriksson, 1988); † A – phlogopite; B, C – biotite; N.A. – not available. Numbers in brackets indicate standard errors.

analysis identifies the micas to be titaniferous phlogopite based on the cationic ratio $Mg/(Mg + Fe^{2+})$ of 0.75 ± 0.2 (Bachinski & Simpson, 1984; Edgar, 1992), with an average BaO content of 1.64% (Table 2), filled tetrahedral and octahedral sites, and deficient interlayer sites. Fluoroapatites contain about 2.5% fluorine.

The Russell Bed contains more elevated K_2O, Al_2O_3 and FeO, and lower SiO_2, CaO and Na_2O percentages, than the bounding shales (Table 1). Elevated FeO and lower SiO_2 percentage in one sample reported here (Table 1) coincide with visible abundance of replacement sulphides. The clay matrix of the Russell Bed is a mixture of illite and smectite (I/S), illite, and kaolinite (Fig. 5). The I/S structure has R3 (ISII) ordering with $> 90\%$ illite based on $\Delta 2\theta = 9.10$, where $\Delta 2\theta$ is the difference between the 001/002 and 002/003 reflections of I/S, calculated to be 7.7 and 16.8 respectively (Moore & Reynolds, 1997). Clay spherules have an I/S composition and a $K_2O\%$ similar to the clay matrix (Table 2).

Standard geochemical proxies used to define characteristics of potential source rocks are illustrated: the ratio pairs Nb/Y–Zr/TiO_2 (Fig. 6), Nb/U–Th/La (Fig. 7), rare earth element (REE) patterns (Fig. 8) and MgO–FeO (Fig. 9). These diagrams compare the ratio pairs with other Ordovician and Silurian North American, British and Scandinavian K-bentonite occurrences.

4.d. Ar–Ar isotope analysis

Phlogopite crystals were analysed from two samples taken near the base (RB) and top (RT) of the Russell Bed. Selected crystals were euhedral and deep orange in colour (plane light), but they possessed dark rims and localized dark intracrystalline discolouration bands. Secondary electronic imaging demonstrates the bands to be sites of replacement chlorite. Similar alteration was noted in biotites from the Lower Silurian Osmundsberg K-bentonite in Europe (Huff *et al.* 1997). Chlorite also forms local interlayer microdomains within the Russell phlogopite crystals.

For sample RB, Ar–Ar analysis produced steeply rising apparent ages with increasing laser power (Fig. 10a). Irregularity of maximum age estimates (Fig. 10a) greater than 420 to 440 Ma (aliquots A through E; Appendix 2) suggests that the age of the crystals is likely older. For sample RT, more consistent near-plateaus occur in the range of 440 to 445 Ma (Fig. 10b). However, individual age estimates range up to 452 Ma (e.g. sample RB, Aliquot A, power 12 in Appendix 2). In summary, the statistical age range is 440–445 Ma. This age is too young compared to that defined globally for the host graptolite *pygmaeus* Zone (451–452 Ma; Webby *et al.* 2004) and may reflect the age of the chlorite alteration.

https://doi.org/10.1017/S001675680400041X Published online by Cambridge University Press

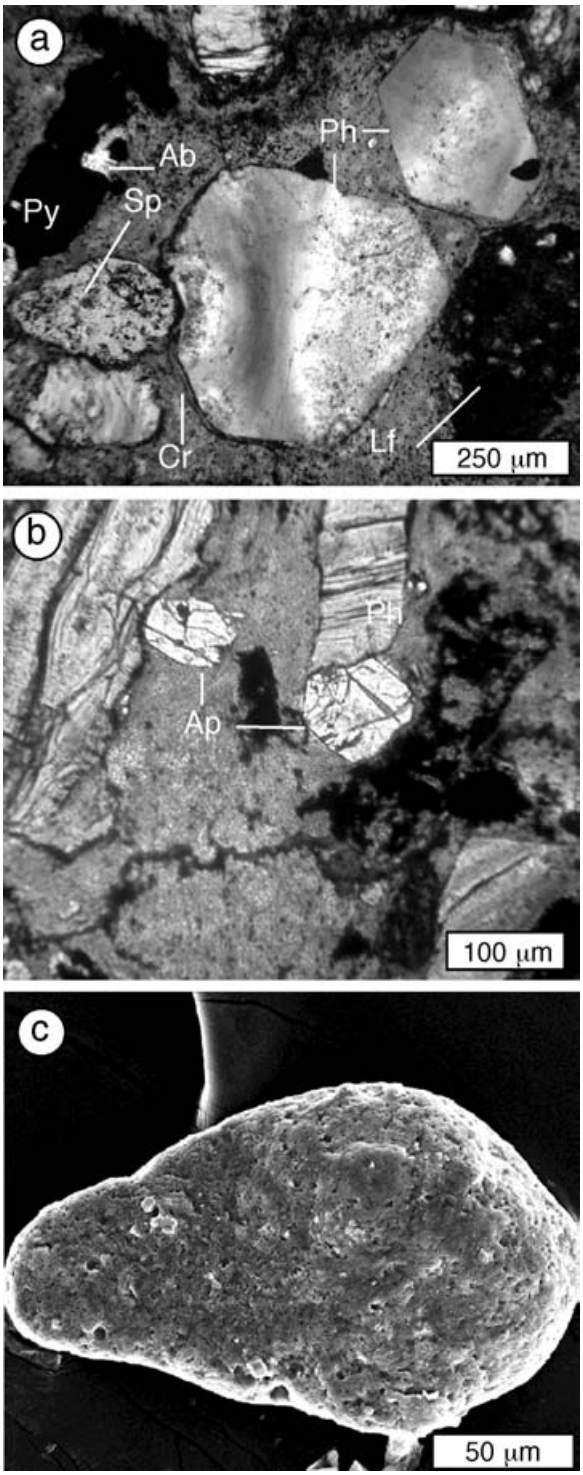

Figure 4. (a) Pseudohexagonal phlogopite (Ph), clay spherules (Sp), mudrock clast (Lf), albite (Ab) replaced by pyrite (Py), and clay rim (Cr) encasing phlogopite phenocryst. Thin-section (plain light) photomicrograph. (b) Phlogopite (Ph), apatite (Ap) phenocrysts in matrix of I/S. Thin-section (plain light) photomicrograph. (c) Teardrop-shaped spherule interpreted as devitrified microspherule. Note the apparent mechanical compaction deformation. Secondary electron microscope image.

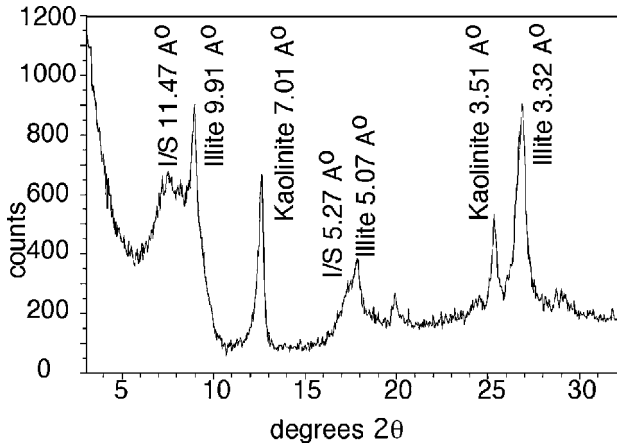

Figure 5. Powder X-ray diffractogram of the < 2 μm size fraction after treating with ethylene glycol. Numbers indicate d-spacing of the peaks.

5. Discussion

5.a. An altered ash bed

Phenocryst texture, presence of clay spherules, mineralogy and elevated K_2O ($\sim 7.5\%$) of the Russell Bed matrix help define this unit as an altered pyroclastic ash deposit, now a K-bentonite. Evidence for mechanical compaction (Fig. 4c) demonstrates post-depositional re-organization of matrix and framework constituents. Fluorapatite and phlogopite phenocrysts are interpreted to define crystal growth and residence time in magma prior to eruption. The few lithic fragments within the deposit represent either xenoliths or reworked mudrock. The clay spherules are of similar shape to, but smaller than, 'Pele's tears' (e.g. Heiken, 1972), or glass droplets associated with volcanic eruptions, notably 'fire fountains'. These constituents are formed rapidly from cooled droplets of magma that take on dynamic shape during transport. Interpreted altered volcanic glass from an Ordovician K-bentonite within the equivalent platform succession along the Cincinnati Arch (Huff & Türkmenoglu, 1981) has similar K_2O of $\sim 7\%$ and SiO_2 of $\sim 50\%$ values as the Russell clay spherules (Table 2). Similarly, the thin rims of clay now found around phlogopite crystals may represent an enveloping microlayer of magma attached to the transported phenocryst. Alternately, these layers identify rapid reworking of phenocrysts after deposition; infolded microlaminae may represent soft-sediment deformation.

The abundant clay matrix and spherules of the Russell K-bentonite are interpreted to be altered devitrified glass. As indicated by a well-known contrast in $K_2O\%$ between Ordovician K-bentonites and Quaternary basaltic glass (Tables 1, 2), the elevated $K_2O\%$ of the clay matrix and spherules is likely due to the fixation of potassium in newly formed clay during conversion of smectite, the initial devitrification product of glass to illite, eventually producing the I/S

https://doi.org/10.1017/S001675680400041X Published online by Cambridge University Press

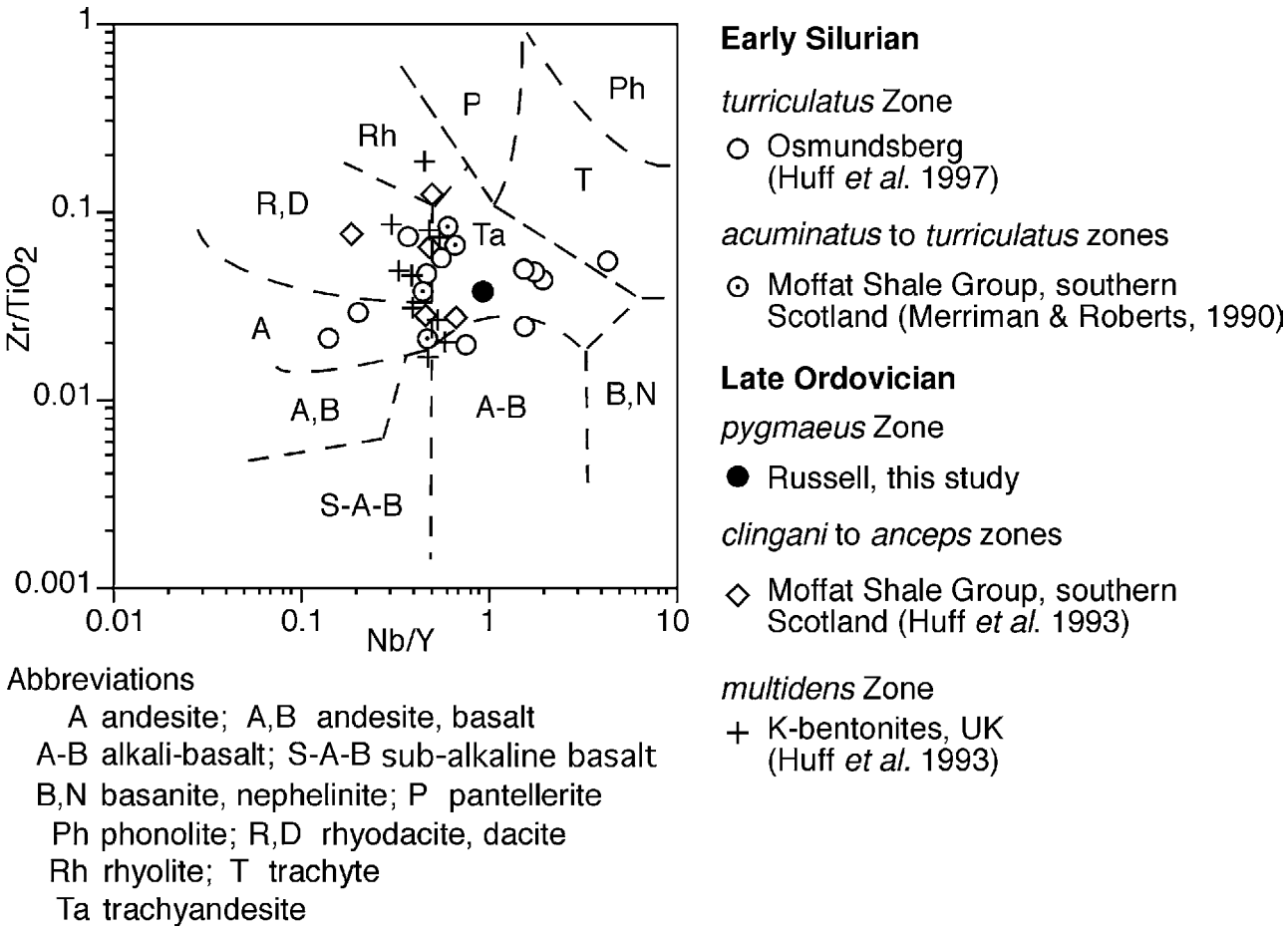

Figure 6. Bulk rock ratios of Nb/Y and Zr/TiO_2 for Late Ordovician and Silurian K-bentonites from North America and the United Kingdom. Dashed lines indicate source fields defined by Winchester & Floyd (1977).

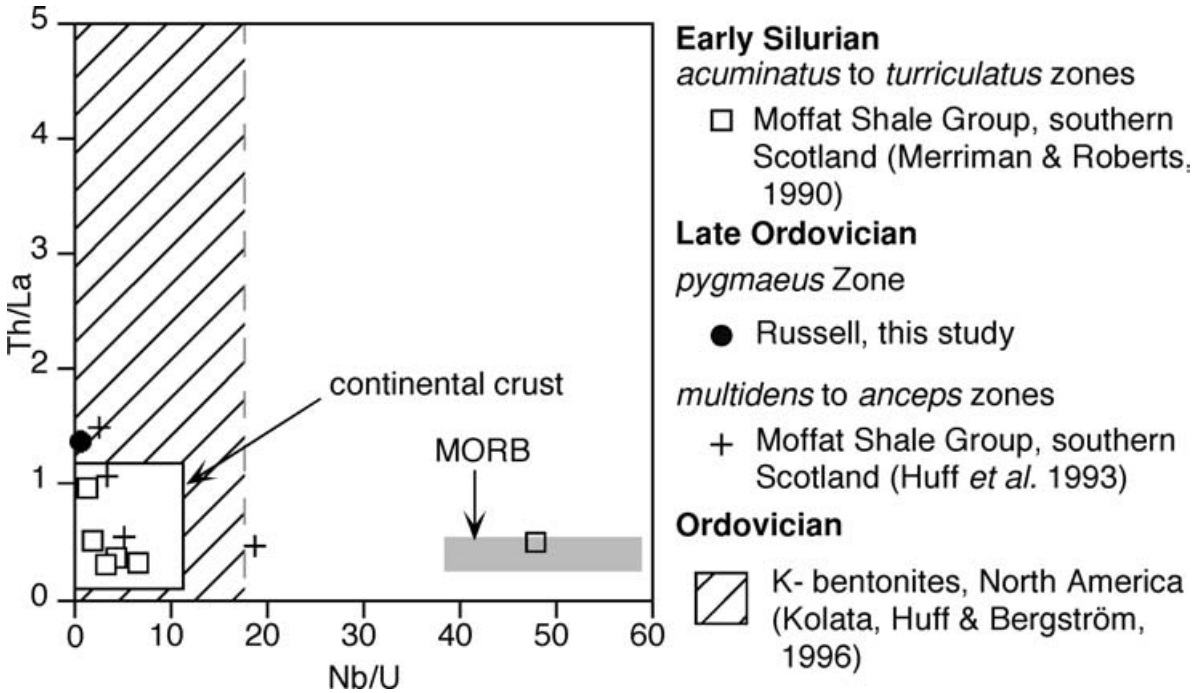

Figure 7. Nb/U–Th/La diagram for the Russell K-bentonite and other Late Ordovician and Early Silurian K-bentonites from North America and the United Kingdom. Fields for Mid-Ocean Ridge Basalt (MORB) and continental crust are from Kolata, Huff & Bergström (1996).

https://doi.org/10.1017/S001675680400041X Published online by Cambridge University Press

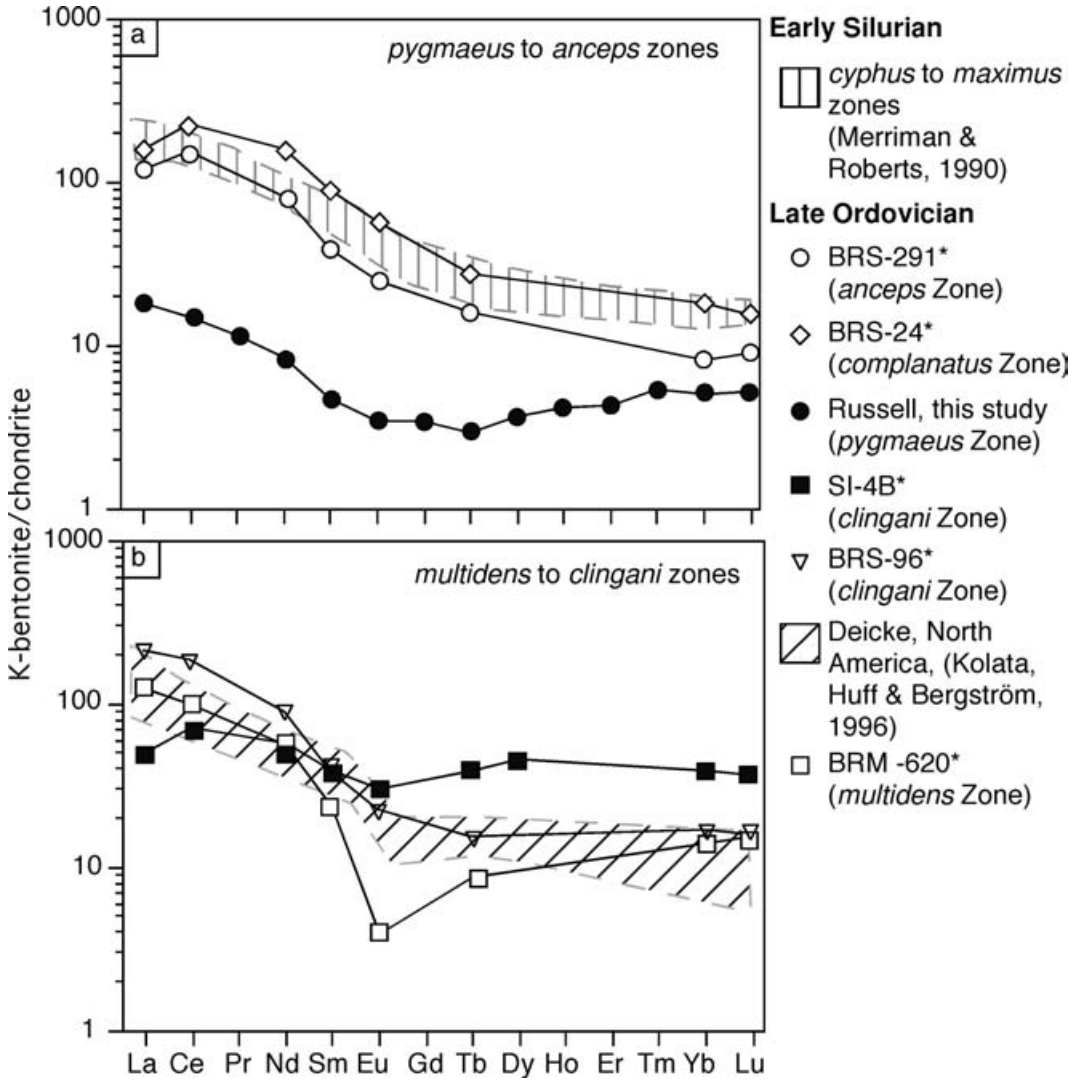

Figure 8. REE of the K-bentonites from eastern North America and the United Kingdom (* indicates data from Huff *et al.* 1993) that post-date (a) and pre-date (b) the Russell Bed.

(Hower *et al.* 1976). This process has not occurred in the bounding shales of the Billings Formation, which possess much lower K_2O% (Table 1), further indicating a unique initial mineralogy for the Russell Bed.

Subsequent diagenetic alteration of this deposit is recognized by the near replacement of smectite by illite, the occurrence of chlorite-altered phlogopite, and the presence of diagenetic sulphides. The presence of R3 I/S with < 10% smectite likely defines smectite to illite diagenesis involving dissolution of I/S and crystallization of illite (Kolata, Huff & Bergström, 1996). This is compatible with a local Conodont Alteration Index (CAI) range of 2.5 to 3 for this part of the basin, or a minimum burial temperature of $> 100\,^{\circ}$C (Legall, Barnes & MacQueen, 1981). Such thermal alteration is also supported by the presence of untwinned euhedral albite in host sediments that likely formed via albitization to near exclusion of other feldspar types (Haynes, 1994). Multi-stage regional and local post-Ordovician hydrothermal activity has been well defined for this basin (Dix & Robinson, 2003). However, further work is necessary to determine the age of the replacement chlorite. Finally, the presence of kaolinite identifies a unique original mineralogy for the Russell Bed. Its presence is rare in Ordovician K-bentonites, but ubiquitous in Early Silurian K-bentonites (Batchelor & Jeppson, 1994). Its presence is a function of availability of potassium during diagenesis and reflects a facies influence (Huff *et al.* 1997).

5.b. Composition of the Russell magmatic source

Bulk rock ratios of Nb/Y and Zr/TiO_2 place the Russell Bed's magmatic source within the trachyandesite field (Fig. 6). The Nb/U–Th/La ratio pair (Fig. 7) identifies a magmatic source that had incorporated a significant component of continental crust and/or oceanic sediment. This association is reinforced by the elevated concentrations of BaO and TiO_2 in phlogopite phenocrysts when compared to most igneous rocks that

https://doi.org/10.1017/S001675680400041X Published online by Cambridge University Press

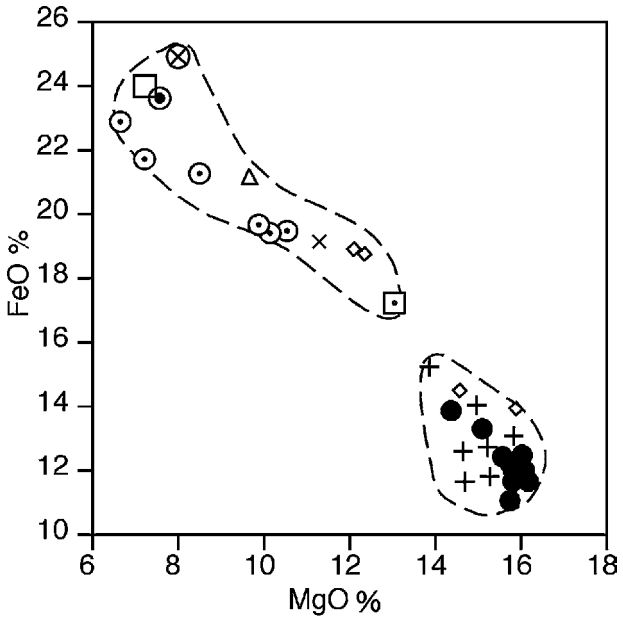

Early Silurian

convolutus to *dubius/nassa* zones

◇ Wenlock, southern Scotland, (Batchelor, 2003)

\+ Llandovery, southern Scotland (Batchelor, 2003)

Late Ordovician

pygmaeus Zone

● Russell , this study

bicornis to *multidens* zones

△ Millbrig, North America (Min, Renne & Huff, 2001)

⊗ Millbrig, North America (Haynes, Melson & Kunk, 1995)

× Deicke, North America (Min, Renne & Huff, 2001)

⊡ Deicke, North America (Haynes, Melson & Kunk, 1995)

⊙ Caradoc, southern Scotland (Batchelor, 2003)

□ Kinnekulle, Sweden (Haynes, Melson & Kunk 1995)

◉ Kinnekulle, Sweden (Min, Renne & Huff, 2001)

Figure 9. MgO and FeO (= total Fe content) for biotites from K-bentonites in North America, southern Scotland and Scandinavia compared to phlogopites in the Russell K-bentonite. Two stratigraphically defined populations are evident: older (> 452 Ma) and younger (< 452 Ma) than the Russell Bed, itself compositionally similar to the younger grouping.

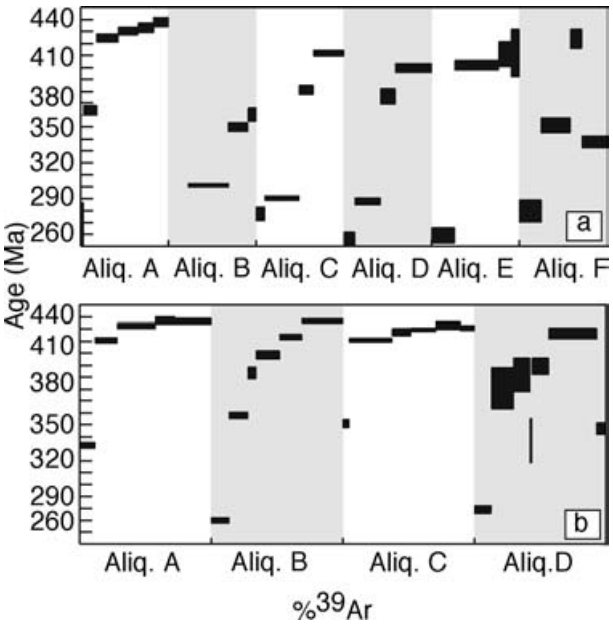

Figure 10. Argon isotopic spectra of gas release for phlogopite phenocrysts. (a) Sample RB. (b) Sample RT. Abbreviation: Aliq. – Aliquot.

have BaO values typically of < 1 % (Speer, 1984). This comparison excludes mantle- or deep crustal-derived potassium-rich sources described by Bachinski & Simpson (1984) and Zhang *et al.* (1993). The above geochemical characteristics suggest the Russell K-bentonite was derived from a silica-poor, mildly alkalic source (cf. Nusbaum, Thayer & Harris, 1988). Similar alkaline, magmatic sources have been interpreted for the Llandovery K-bentonites from Europe (Batchelor & Jeppsson, 1994).

Compositionally, the Russell Bed has greater affinity with younger (Silurian) deposits in Scotland and Scandinavia than the older Ordovician K-bentonites in eastern North America or Europe. For example, the MgO–FeO pair and cationic ratio $Mg/(Mg+Fe^{2+})$ of the phlogopite phenocrysts further help to identify the extent of magmatic fractionation (Fig. 9). MgO is concentrated in less fractionated melts whereas FeO accumulates in more fractionated magmas (Batchelor, 2003). The Deicke, Millbrig and Kinnekulle K-bentonites of eastern North America and Europe show $Mg/(Mg+Fe^{2+})$ ratio ranges of 0.59–0.64, 0.44–0.54 and 0.43–0.44, respectively (Haynes, Melson & Kunk, 1995; Min, Renne & Huff, 2001). In comparison, the Russell Bed and the Llandlovery K-bentonites from Europe yield values of 0.75 ± 0.2, and 0.73 ± 0.03 (Batchelor, 2003), respectively. This distinction suggests that the magmatic sources for these volcanic events were less fractionated than the older more acidic eruptives. A more mafic magmatic source for the Russell Bed is supported by the presence of altered devitrified dynamically glass spherules. Their formation is usually taken to define a low-viscosity, on the order of 10^{6-7} poise, fluid-rich mafic

https://doi.org/10.1017/S001675680400041X Published online by Cambridge University Press

magmatic source (Heiken, 1972; Melson, O'Hearn & Fredriksson, 1988). These constituents have not been documented previously from Ordovician K-bentonites in eastern North America. Instead, altered glass shards have been reported from the Millbrig deposit (Haynes, 1992); this form is in keeping with a more acidic magmatism.

K-bentonites in Baltica and eastern Laurentia older than the Russell Bed (for example, within the *bicornis* to *spiniferus* graptolite zones, ~ 458 to 452 Ma; Webby *et al.* 2004) also define predominantly rhyolitic, rhyodacitic and andesitic sources (Fig. 6). K-bentonites younger than the Russell Bed within the Early Silurian shale/limestone successions of Scotland and Scandinavia identify acidic to intermediate, andesite, trachyandesite and trachyte sources (Fig. 6). Some overlap is evident. Light REE enrichment of the Russell Bed is calculated to be $La_N/Yb_N = 3.1$, compared to $La_N/Yb_N = 11.2$ for Deicke and $La_N/Yb_N = 9.1$ for Millbrig K-bentonite (Kolata, Huff & Bergström, 1996). When coupled with a Eu/Eu* ratio of ~ 0.85, the magmatic source for the Russell Bed was less fractionated (Table 1). REE patterns for Late Ordovician to Early Silurian K-bentonites in eastern Laurentia and Baltica demonstrate loss of the prominent Eu* anomaly that characterizes the older platform-hosted deposits (Fig. 8b). Thus, accounting for sediment dilution, the REE pattern for the Russell Bed has a greater affinity with Early Silurian deposits in Europe (Fig. 8a).

The potassic nature of the Russell Bed and the Early Silurian K-bentonites of Europe may be attributed to sources derived from a waning subduction zone, in which there was increased incorporation of crustal material during continental collision (Batchelor & Jeppsson, 1994). Such a mechanism has been well documented from the Quaternary history of Stromboli (Batchelor & Jeppsson, 1994).

5.c. Plinian-scale or basin-restricted eruption?

The Russell Bed's significance in defining a regional and temporal transition in magmatic composition awaits further study of other deposits in the Taconic shale basins. Nevertheless, the timing of volcanism following platform collapse suggests that potential change in magmatic sources (as suggested by compositional similarity with Silurian deposits) may well be associated with regional basin re-organization.

If gamma ray well logs define a regional distribution for the Russell K-bentonite (Fig. 3), deposition of volcanic ash was widespread (2×10^5 km^2; Fig. 2) within a deep-water basin. The present thickness (6 cm) of the Russell Bed defines a significant volume of ash transported through the water column. Glass spherules of airfall origin have been documented in much deeper water settings, for example, in Tertiary pelagic clay from the eastern Pacific Ocean basin (Vallier *et al.* 1977; Melson, O'Hearn & Fredriksson, 1988). Assuming an airfall origin for the Russell K-bentonite, a possible minimum plume transport distance of 250 to 750 km is estimated on the basis of phenocryst size (Fisher & Schmincke, 1984; pp. 173–6). As with interpretations for the older Appalachian K-bentonites, an Appalachian source is plausible incorporating southeasterly to northwesterly palaeowind directions (Kolata, Huff & Bergström, 1996). More distal sources could exist with stratospheric circulation (Delano *et al.* 1990).

If, however, the individual gamma ray deflections (Fig. 3) correspond to separate deposits closely positioned in space and time, the Russell K-bentonite defines an intrabasinal occurrence. Thus, we cannot exclude a submarine fire fountain eruption, where glass spheres and globules are common occurrences (Simpson & McPhie, 2001). Such eruptions are commonplace along volcanic arcs in water depths of 200–500 m, or > 1000 m, if gas-rich (Carey, 2000). The water depth of the lower Billings Formation was bathyal (Sharma, Dix & Riva, 2003).

Whether of local or regional distribution, volcanism coincided with two other significant geological events in the basin. First, it immediately pre-dates initial influx of distal turbidites that, elsewhere along the orogen, correspond to the initial stages of Taconic foreland flysch (Hiscott, Pickering & Beeden, 1986). With this change came abrupt deep-water ventilation of the basin (Sharma, Dix & Riva, 2003), possibly due to downwelling of the dense oxygenated surface water. Second, the eruption coincides with intrabasinal extinction of four graptolite species (Sharma, Dix & Riva, 2003). Productivity may have been greatly affected by ash transported through the water column or an attendant change in seawater chemistry.

In summary, the Russell Bed documents more than a product of an occasional eruption. Its stratigraphic position underscores connectivity among volcanism, possible temporal change in magmatic source allied to orogenic activity, palaeoceanographic effects, and influx of turbidites. This deposit coincided with onset of a new era of basin-fill for this specific Taconic basin.

6. Conclusions

The Russell K-bentonite represents accumulation of volcanic ash within a deep-water shale basin of Late Ordovician (451–452 Ma) age. Predominant framework constituents of this clay-rich, mostly I/S with > 90% illite, sediment are titaniferous phlogopite with 1.6% BaO, fluoroapatite and altered glass spherules. Geochemical proxies, and the presence of clay-altered glass spherules, support a mildly alkaline, intermediate, trachyandesitic, magmatic source that incorporated a significant component of oceanic sediment and/or continental crust, recording the waning stage of a

https://doi.org/10.1017/S001675680400041X Published online by Cambridge University Press

subduction zone prior to continental collision. The Russell Bed immediately precedes arrival of distal turbidites, which in turn brought profound palaeoceanographic changes to the basin. Further study is necessary to determine how regional this event may have been, and the potential tectonic interconnectivity among adjacent Taconic basins.

Acknowledgements. This work represents part of S. Sharma's doctoral research supported by a Natural Sciences and Engineering Research Council Discovery Grant to G. R. Dix. We thank the Geological Survey of Canada (GSC) for permission to sample the Russell No. 2 core. B. Cousens, D. Hogarth, I. Jonasson, A. Lalonde and R. Taylor are thanked for discussions regarding volcanic processes and petrology. We thank referees W. D. Huff and D. Wray for their suggestions.

References

BACHINSKI, S. W. & SIMPSON, E. L. 1984. Ti-phlogopites of the Shaw's Cove minette: a comparison with micas of other lamprophyres, potassic rocks, kimberlites and mantle xenoliths. *American Mineralogist* **69**, 41–56.

BAIRD, G. C. & BRETT, C. E. 2002. Indian Castle Shale: late synorogenic siliciclastics succession in an evolving Middle to Late Ordovician foreland basin, eastern New York State. *Physics and Chemistry of the Earth* **27**, 203–30.

BATCHELOR, R. A. 2003. Geochemistry of biotite in metabentonites as age discriminant, indicator of regional magma sources and potential correlating tool. *Mineralogical Magazine* **67**, 807–17.

BATCHELOR, R. A., HARPER, D. A. T. & ANDERSON, T. B. 2003. Geochemistry and potential correlation of Silurian (Telychian) metabentonites from Ireland and SW Scotland. *Geological Journal* **38**, 161–74.

BATCHELOR, R. A. & JEPPSON, L. 1994. Late Llandovery bentonites from Gotland, Sweden, as chemostratigraphic markers. *Journal of Geological Society, London* **151**, 741–6.

BATCHELOR, R. A. & WEIR, J. A. 1988. Metabentonite geochemistry: magmatic cycles and graptolite extinctions at Dob's Linn, Southern Scotland. *Transactions of the Royal Society of Edinburgh, Earth Sciences* **79**, 19–41.

BERGSTRÖM, S. M., HUFF, W. D., KOLATA, D. & MELCHIN, M. J. 1997. Occurrence and significance of Silurian K-bentonite beds at Arisaig, Nova Scotia, eastern Canada. *Canadian Journal of Earth Sciences* **34**, 1630–43.

BERGSTRÖM, S. M. & MITCHELL, C. E. 1994. Regional relationships between late Middle and early Late Ordovician standard successions in New York and Quebec and the Cincinnati region in Ohio, Indiana, and Kentucky. In *Studies in stratigraphy and paleontology in honor of Donald W. Fisher* (ed. E. Landing), pp. 5–20. New York State Museum Bulletin 481.

CAREY, S. 2000. Volcaniclastic sedimentation around island arcs. In *Encyclopedia of Volcanoes* (ed. M. Sigurdsson), pp. 627–42. San Diego, USA Academic Press.

CLARK, T. H. & STEVENSON, J. S. 1960. Authigenic biotite in the Utical shale at L'Eppiphanie, Quebec. *Geological Association of Canada Proceedings* **12**, 97–104.

DAVIES, S. M., TURNEY, C. S. M. & LOWE, J. J. 2001. Identification and significance of a visible, basalt-rich Vedde Ash layer in a Late-glacial sequence on the Isle of Skye, Inner Hebrides, Scotland. *Journal of Quaternary Science* **16**, 99–104.

DELANO, J. W., SCHIRNICK, C., BOCK, B., KIDD, W. S. F., HEIZLER, M. T., PUTMAN, G. W., DE LONG, S. E. & OHR, M. 1990. Petrology and geochemistry of Ordovician K-bentonites in New York State: Constraints on the nature of a volcanic arc. *Journal of Geology* **98**, 157–70.

DELANO, J. W., TICE, S. J., MITCHELL, C. E. & GOLDMAN, D. 1994. Rhyolitic glass in Ordovician K-bentonites: A new stratigraphic tool. *Geology* **22**, 115–8.

DIECCHIO, R. J. 1991. Taconian sedimentary basins of the Appalachians. In *Advances in Ordovician Geology* (eds C. R. Barnes and S. H. Williams), pp. 225–34. Geological Survey of Canada Paper 90-9.

DIX, G. R. & ROBINSON, G. W. 2003. The geochemical record of hydrothermal mineralization and tectonism inboard of the Appalachian Orogen: the Ottawa Embayment. *Chemical Geology* **197**, 29–53.

EDGAR, A. D. 1992. Barium-rich phlogopite and biotite from some Quaternary alkali mafic lavas, West Eifel, Germany. *European Journal of Mineralogy* **4**, 321–30.

FISHER, R. V. & SCHMINCKE, H.-U. 1984. *Pyroclastic Rocks*. Heidelberg, Germany: Springer-Verlag, 472 pp.

HAYNES, J. T. 1992. Reinterpretation of Rocklandian (Upper Ordovician) K-bentonite stratigraphy in southwest Virginia, southeast west Virginia, and northeast Tennessee. *Virginian Division of Mineral Resources Publication* **126**, 58 pp.

HAYNES, J. T. 1994. The Ordovician Deicke and Millbrig K-Bentonite Beds of the Cincinnati Arch and the Southern Valley and Ridge Province. *Geological Society of America Special Paper* **290**, 80 pp.

HAYNES, J. T., MELSON, W. G. & KUNK, M. J. 1995. Composition of biotite phenocrysts in Ordovician tephras casts doubt on the proposed trans-Atlantic correlation of the Millbrig K-bentonite (United States) and the Kinnekulle K-bentonite (Sweden). *Geology* **23**, 847–50.

HEIKEN, G. 1972. Morphology and Petrography of Volcanic Ashes. *Geological Society of America Bulletin* **83**, 1961–88.

HISCOTT, R. N., PICKERING, K. T. & BEEDEN, D. R. 1986. Progressive filling of a confined Middle Ordovician foreland basin associated with the Taconic Orogeny, Quebec, Canada. *Special Publication International Association of Sedimentologists* **8**, 309–25.

HOWER, J., ESLINGER, E. V., HOWER, M. E. & PERRY, E. A. 1976. Mechanism of burial metamorphism of argillaceous sediment: 1. Mineralogical and chemical evidence. *Geological Society of America Bulletin* **87**, 725–37.

HUFF, W. D., BERGSTRÖM, S. M., KOLATA, D. R. & SUN, H. 1997. The Lower Silurian Osmundsberg K-bentonite. Part II: mineralogy, geochemistry, chemostratigraphy and tectonomagmatic significance. *Geological Magazine* **135**, 15–26.

HUFF, W. D., MERRIMAN, R. J., MORGAN, D. J. & ROBERTS, B. 1993. Distribution and tectonic setting of Ordovician K-bentonites in the United Kingdom. *Geological Magazine* **130**, 93–100.

HUFF, W. D. & TÜRKMENOGLU, A. G. 1981. Chemical characteristics and origin of Ordovician K-bentonites along the Cincinnati Arch. *Clays and Clay Minerals* **29**, 113–23.

KOLATA, D. R., FROST, J. K. & HUFF, W. D. 1986. K-bentonites of the Ordovician Decorah Subgroup, Upper Mississippi Valley: Correlation by chemical fingerprinting. *Illinois State Geological Survey Circular* **537**, 1–30.

KOLATA, D. R., HUFF, W. D. & BERGSTRÖM, S. M. 1996. Ordovician K-bentonites of eastern North America. *Geological Society of America Special Paper* **313**, 1–84.

LEGALL, F. D., BARNES, C. R. & MACQUEEN, R. 1981. Thermal maturation, burial history and hotspot development, Palaeozoic strata of southern Ontario–Quebec, from conodont and acritarch colour alteration studies. *Bulletin of Canadian Petroleum Geology* **29**, 492–539.

MCKERROW, W. S., DEWEY, J. F. & SCOTESE, S. R. 1991. The Ordovician and Silurian development of the Iaepetus Ocean. *Special Papers in Palaeontology* **44**, 165–78.

MELSON, W. G., O'HEARN, T. & FREDRIKSSON, K. 1988. Composition and origin of basaltic glass spherules in pelagic clay from the eastern Pacific. *Marine Geology* **83**, 253–71.

MERRIMAN, R. J. & ROBERTS, B. 1990. Metabentonites in the Moffat Shale Group, Southern Uplands of Scotland: Geochemical evidence of ensialic marginal basin volcanism. *Geological Magazine* **127**, 259–71.

MIN, K., RENNE, P. R. & HUFF, W. D. 2001. $^{40}Ar/^{39}Ar$ dating of Ordovician K-bentonites in Laurentia and Baltoscandia. *Earth and Planetary Science Letters* **185**, 121–34.

MOORE, D. M. & REYNOLDS, R. C. JR. 1997. *X-Ray Diffraction and the Identification and Analysis of Clay Minerals*, 2nd ed. New York: Oxford University Press, 378 pp.

NUSBAUM, R. L., THAYER, P. T. & HARRIS, W. B. 1988. Source constraints based on biotite analysis for the 47 Ma Castle Hayne bentonite, North Carolina. *Southeastern Geology* **29**, 29–39.

RENNE, P. R., SWISHER, C. C., DEINO, A. L., KARNER, D. B., OWENS, T. L. & DEPAOLO, D. J. 1998. Intercalibration of standards, absolute ages and uncertainties in $^{40}Ar/^{39}Ar$ dating. *Chemical Geology* **145**, 117–52.

RODDICK, J. C. 1988. The assessment of errors in $^{40}Ar/^{39}Ar$ dating. In *Radiogenic Age and Isotopic Studies, Report 2*, pp. 7–16. Geological Survey of Canada Paper no. 88-2.

SAMSON, S. D., KYLE, P. R. & ALEXANDER, E. C. JR. 1988. Correlation of North American Ordovician bentonites by using apatite chemistry. *Geology* **16**, 444–7.

SANFORD, B. V. 1993. St. Lawrence Platform-Geology. In *Sedimentary cover of the craton in Canada* (eds D. F. Stott and J. D. Aitken), pp. 723–86. Geological Survey of Canada, Geology of Canada no. 5.

SHARMA, S. & DIX, G. R. 2004. Magnesian calcite and chamositic ooids forming shoals peripheral to Late Ordovician (Ashgill) muddy siliciclastic shores: southern Ontario. *Palaeogeography, Palaeoclimatology, Palaeoecology* **210**, 349–68.

SHARMA, S., DIX, G. R. & RIVA, J. F. V. 2003. Late Ordovician platform foundering, its paleoceanography and burial, as preserved in separate (eastern Michigan Basin, Ottawa Embayment) basins, southern Ontario. *Canadian Journal of Earth Sciences* **40**, 135–48.

SIMPSON, K. & MCPHIE, J. 2001. Fluidal-clast breccia generated by submarine fire fountaining, Tropper Creek Formation, Queensland, Australia. *Journal of Volcanology and Geothermal Research* **109**, 339–55.

SPEER, J. A. 1984. Micas in igneous rocks. In *Micas* (ed. S. W. Bailey), pp. 299–349. *Reviews in Mineralogy* **13**. Mineralogical Society of America.

TREVAIL, R. A. 1990. Ordovician bentonites in the subsurface of southwestern Ontario. In *29th Annual Conference Proceedings*, Ontario Petroleum Institute, 18 pp.

VALLIER, T. L., BOHRER, D., GROVER, M. & MCKEE, E. 1977. Origin of basalt microlapilli in lower Miocene pelagic sediment, northeastern Pacific Ocean. *Geological Society of America Bulletin* **88**, 787–96.

VILLENEUVE, M. E. & MACINTYRE, D. G. 1997. Laser $^{40}Ar/^{39}Ar$ ages of the Babine Porphyries and Newman Volcanics, Fulton Lake map area, west-central British Columbia. In *Radiogenic Age and Isotopic Studies, Report 10*, pp. 131–9. Geological Survey of Canada, Current Research 1997-F.

VILLENEUVE, M. E., SANDEMAN, H. A. & DAVIS, W. J. 2000. A method for the intercalibration of U–Th–Pb and $^{40}Ar/^{39}Ar$ ages in the Phanerozoic. *Geochimica et Cosmochimica Acta* **64**, 4017–30.

WEBBY, B. D., COOPER, R. A., BERGSTRÖM, S. M. & PARIS, F. 2004. Stratigraphic Framework and Time Slices. In *The Great Ordovician Biodeversification Event* (eds B. D. Webby, F. Paris, M. L. Droser and I. G. Percival), pp. 41–7. New York: Columbia University Press.

WINCHESTER, J. A. & FLOYD, P. A. 1977. Geochemical discrimination of different magma series and their differentiation products using immobile elements. *Chemical Geology* **20**, 325–43.

WOODCOCK, N. H. 2000. Introduction to the Silurian. In *British Silurian stratigraphy* (ed. L. P. Thomas), pp. 1–22. *Geological Conservation Series* **19**.

ZHANG, M., SUDDABY, P., THOMPSON, R. N. & DUNGAN, M. 1993. Barium titanium phlogopite from potassic lavas in northeast China: chemistry, substitutions, and paragenesis. *American Mineralogist* **78**, 1056–65.

Appendix 1. Ar–Ar analytical techniques

Individual crystals used in this analysis varied in size from 0.5 to 1 mm, and were hand-picked from water-disaggregated whole rock samples. Individual mineral separates were loaded into aluminium foil packets along with a single grain of Fish Canyon Tuff Sanidine (FCT-SAN) to act as flux monitor (apparent age = 28.02 ± 0.28 Ma: Renne *et al.* 1998). The sample packets were arranged radially inside an aluminium can. The samples were then irradiated for 12 hours at McMaster University in a fast neutron flux of approximately 3×10^{16} neutrons/cm^2. Samples were then split into several aliquots and loaded into individual 1.5 mm diameter holes in a copper planchet. The planchet was placed in the extraction line and the system evacuated. Heating of individual sample aliquots in steps of increasing temperature was achieved using a Merchantek MIR10 10W CO_2 laser equipped with a 2 mm × 2 mm flat-field lens. Ar gas released by this process was cleaned over getters for ten minutes, then analysed isotopically using the secondary electron multiplier system of a VG3600 gas source mass spectrometer. Details of data collection protocols can be found in Villeneuve & MacIntyre (1997) and Villeneuve, Sandeman & Davis, (2000).

https://doi.org/10.1017/S001675680400041X Published online by Cambridge University Press

Corrected argon isotopic data are listed in Appendix 2, and presented as spectra of gas release plots (Fig. 10). These spectra contain step heating data from multiple aliquots, plotted side-by-side and alternately shaded. These types of plots provide a visual image of replicated heating profiles, the error and apparent age of each step, and evidence for loss of Ar in the low-temperature steps.

Neutron flux gradients throughout the sample canister were evaluated by analysing the FCT-SAN flux monitors included with each sample packet and interpolating a linear fit against calculated J-factor and sample position. The error on individual J-factor values is conservatively estimated at $\pm 0.6\%$ (2σ). Because the error associated with the J-factor is systematic and not related to individual analyses, correction for this uncertainty is not applied until calculation of dates from isotopic correlation diagrams (Roddick, 1988). No evidence for excess ^{40}Ar was observed in any of the samples and, therefore, all regressions are assumed to pass through the $^{40}Ar/^{36}Ar$ value for atmospheric air (295.5). All errors are quoted at the 2σ level of uncertainty.

Appendix 2. Ar–Ar data for phlogopites from Russell K-bentonite

P*	Vol. ^{39}Ar $\times 10^{-11}$cc	$^{36}Ar/^{39}Ar$	$^{37}Ar/^{39}Ar$	$^{38}Ar/^{39}Ar$	$^{40}Ar/^{39}Ar$	%^{40}Ar ATM	$*^{40}Ar/^{39}Ar$	$f^{\dagger}_{39}$ (%)	Apparent age (Ma)§
RB Phlogopite J = .00289650 Billings Formation# (Z7700; 45.3132°N 75.3904°E)									
Aliquot: A									
2.4	0.2208	0.3660 ± 0.0182	0.098 ± 0.016	0.083 ± 0.015	174.886 ± 7.246	67.3	57.196 ± 4.447	0.8	276.55 ± 19.94
3	1.0956	0.0023 ± 0.0028	0.014 ± 0.003	0.049 ± 0.011	80.354 ± 0.958	0.9	79.609 ± 1.012	4.2	374.33 ± 4.30
3.9	1.7877	0.0010 ± 0.0018	0.013 ± 0.002	0.062 ± 0.011	94.378 ± 0.816	0.3	94.054 ± 0.849	6.8	434.65 ± 3.49
4.6	1.5808	0.0014 ± 0.0019	0.027 ± 0.002	0.066 ± 0.011	95.930 ± 0.780	0.5	95.478 ± 0.815	6.0	440.49 ± 3.34
5.5	1.2927	0.0006 ± 0.0024	0.015 ± 0.003	0.066 ± 0.011	96.348 ± 0.917	0.3	96.104 ± 0.968	4.9	443.05 ± 3.96
12	1.165	0.0010 ± 0.0027	0.017 ± 0.002	0.067 ± 0.011	97.653 ± 0.986	0.4	97.288 ± 1.044	4.4	447.88 ± 4.26
Aliquot: B									
3	1.5779	0.0078 ± 0.0020	0.029 ± 0.003	0.032 ± 0.011	52.559 ± 0.461	4.5	50.188 ± 0.515	6.0	244.86 ± 2.35
4.6	3.1811	0.0019 ± 0.0010	0.008 ± 0.001	0.030 ± 0.011	65.579 ± 0.347	0.9	64.982 ± 0.37	12.1	311.12 ± 1.63
5.5	1.5611	0.0007 ± 0.0020	0.015 ± 0.002	0.049 ± 0.011	76.495 ± 0.869	0.3	76.246 ± 0.901	6.0	359.99 ± 3.86
12	0.6389	0.0016 ± 0.0048	0.030 ± 0.004	0.057 ± 0.012	79.305 ± 1.174	0.7	78.714 ± 1.341	2.4	370.53 ± 5.71
Aliquot: C									
3	0.6813	0.0390 ± 0.0050	0.035 ± 0.002	0.065 ± 0.011	71.482 ± 1.064	16.7	59.546 ± 1.288	2.6	287.06 ± 5.74
4.6	2.5896	0.0072 ± 0.0013	0.012 ± 0.001	0.031 ± 0.011	64.727 ± 0.392	3.4	62.551 ± 0.425	9.9	300.40 ± 1.88
5.5	1.1137	0.0018 ± 0.0027	0.042 ± 0.002	0.052 ± 0.011	84.239 ± 0.877	0.7	83.641 ± 0.940	4.2	391.37 ± 3.96
12	2.2754	0.0007 ± 0.0014	0.056 ± 0.002	0.063 ± 0.011	91.250 ± 0.605	0.3	91.020 ± 0.641	8.7	422.15 ± 2.65
Aliquot: D									
3	0.5135	0.1747 ± 0.0084	0.068 ± 0.044	0.068 ± 0.012	107.620 ± 2.356	49.9	53.970 ± 2.174	2	262.03 ± 9.83
4.6	1.1912	0.0102 ± 0.0026	0.066 ± 0.020	0.030 ± 0.011	65.046 ± 0.660	4.8	61.933 ± 0.715	4.5	297.67 ± 3.17
5.5	0.6994	0.0053 ± 0.0046	0.101 ± 0.032	0.037 ± 0.012	84.059 ± 1.421	2	82.367 ± 1.568	2.7	386.00 ± 6.62
12	1.654	0.0018 ± 0.0019	0.035 ± 0.019	0.059 ± 0.011	88.549 ± 0.820	0.7	87.970 ± 0.864	6.3	409.49 ± 3.60
Aliquot: E									
3	0.3837	0.0288 ± 0.0042	0.218 ± 0.061	0.042 ± 0.012	64.022 ± 0.968	13.3	55.497 ± 1.426	1.5	268.92 ± 6.42
4.6	0.7013	0.0019 ± 0.0022	0.076 ± 0.058	0.056 ± 0.011	89.110 ± 0.833	0.6	88.536 ± 1.010	2.7	411.84 ± 4.20
5.5	0.2088	0.0046 ± 0.0071	0.132 ± 0.159	0.068 ± 0.013	92.178 ± 1.704	1.5	90.786 ± 2.513	0.8	421.18 ± 10.40
12	0.1325	0.0054 ± 0.0125	0.315 ± 0.181	0.086 ± 0.018	92.649 ± 3.562	1.8	91.024 ± 4.872	0.5	422.16 ± 20.15
Aliquot: F									
3	0.355	0.0801 ± 0.0066	0.303 ± 0.093	0.070 ± 0.013	83.828 ± 1.322	28.2	60.162 ± 2.106	1.3	289.80 ± 9.37
4.6	0.4605	0.0038 ± 0.0030	0.140 ± 0.060	0.027 ± 0.012	77.715 ± 1.303	1.5	76.585 ± 1.500	1.7	361.44 ± 6.42
5.5	0.1826	−0.0001 ± 0.0000	0.352 ± 0.120	0.052 ± 0.014	92.808 ± 1.938	−1.2	93.914 ± 1.955	0.7	434.07 ± 8.03
12	0.3979	0.0017 ± 0.0029	0.235 ± 0.051	0.047 ± 0.011	73.949 ± 0.908	0.7	73.430 ± 1.154	1.4	347.90 ± 4.97
RT Phlogopite; J = .00290220 Billings Formation (Z7657; 45.3132°N 75.3904°E)									
Aliquot: A									
3	2.2027	0.0052 ± 0.0012	0.011 ± 0.001	0.050 ± 0.011	73.495 ± 0.587	2	72.036 ± 0.616	4.4	342.50 ± 2.67
3.9	3.1977	0.0008 ± 0.0008	0.011 ± 0.001	0.057 ± 0.011	93.088 ± 0.534	0.2	92.922 ± 0.549	6.4	430.75 ± 2.26
4.6	5.4968	0.0002 ± 0.0004	0.006 ± 0.001	0.060 ± 0.011	95.854 ± 0.595	0	95.817 ± 0.601	11	442.65 ± 2.46
5	2.7617	0.0007 ± 0.0009	0.010 ± 0.002	0.063 ± 0.011	97.032 ± 0.745	0.1	96.907 ± 0.763	5.5	447.11 ± 3.12
6	2.8177	0.0005 ± 0.0010	0.004 ± 0.002	0.066 ± 0.011	96.819 ± 0.649	0.1	96.743 ± 0.686	5.6	446.43 ± 2.81
12	2.4583	0.0006 ± 0.0010	0.009 ± 0.001	0.061 ± 0.011	96.874 ± 0.653	0.1	96.760 ± 0.674	4.9	446.51 ± 2.76
Aliquot: B									
3	1.8144	0.0109 ± 0.0021	0.022 ± 0.001	0.035 ± 0.011	61.272 ± 0.502	5.6	57.838 ± 0.519	3.6	279.94 ± 2.33
3.9	1.8721	0.0034 ± 0.0021	0.017 ± 0.002	0.053 ± 0.011	79.105 ± 0.636	1.5	77.924 ± 0.672	3.7	367.81 ± 2.87
4.2	0.8887	0.0019 ± 0.0043	0.031 ± 0.003	0.076 ± 0.012	87.306 ± 1.152	1.1	86.366 ± 1.216	1.8	403.51 ± 5.09
5	2.3407	0.0000 ± 0.0019	0.040 ± 0.002	0.072 ± 0.011	90.079 ± 0.826	0.2	89.940 ± 0.853	4.7	418.41 ± 3.54
6	2.2764	0.0003 ± 0.0017	0.111 ± 0.003	0.093 ± 0.012	93.871 ± 0.573	0.3	93.632 ± 0.597	4.5	433.67 ± 2.46
12	4.1385	0.0001 ± 0.0008	0.046 ± 0.003	0.087 ± 0.011	96.819 ± 0.495	0	96.776 ± 0.509	8.3	446.57 ± 2.08

https://doi.org/10.1017/S001675680400041X Published online by Cambridge University Press

Appendix 2. *Continued*

P*	Vol. ^{39}Ar $\times 10^{-11}$cc	^{36}Ar/^{39}Ar	^{37}Ar/^{39}Ar	^{38}Ar/^{39}Ar	^{40}Ar/^{39}Ar	%^{40}Ar ATM	*^{40}Ar/^{39}Ar	$f_{39}^{\dagger}$ (%)	Apparent age (Ma)§
Aliquot: C									
3	0.5279	0.0133 ± 0.0017	0.013 ± 0.004	0.064 ± 0.011	80.264 ± 0.836	4.9	76.328 ± 0.872	1.1	360.99 ± 3.74
3.9	3.3323	0.0012 ± 0.0005	0.004 ± 0.001	0.063 ± 0.011	93.290 ± 0.386	0.4	92.943 ± 0.407	6.7	430.83 ± 1.68
4.2	1.5178	0.0012 ± 0.0011	0.004 ± 0.002	0.064 ± 0.011	94.913 ± 0.758	0.4	94.549 ± 0.807	3	437.45 ± 3.32
5	1.9994	0.0009 ± 0.0006	0.012 ± 0.002	0.069 ± 0.011	95.375 ± 0.347	0.3	95.095 ± 0.379	4	439.69 ± 1.56
6	1.9238	0.0006 ± 0.0008	0.002 ± 0.002	0.064 ± 0.011	96.036 ± 0.791	0.2	95.851 ± 0.822	3.8	442.79 ± 3.37
12	1.1054	0.0029 ± 0.0009	0.005 ± 0.004	0.072 ± 0.011	96.249 ± 0.518	0.9	95.380 ± 0.546	2.2	440.85 ± 2.24
Aliquot: D									
15	0.4974	0.0164 ± 0.0030	0.528 ± 0.131	0.074 ± 0.011	80.242 ± 0.899	6.1	75.377 ± 1.168	1	356.90 ± 5.02
3	0.9449	0.0449 ± 0.0017	0.214 ± 0.060	0.037 ± 0.011	73.127 ± 0.671	18.2	59.853 ± 0.727	1.9	288.95 ± 3.24
3.9	1.2662	0.0039 ± 0.0007	0.069 ± 0.020	0.048 ± 0.060	84.438 ± 4.152	1.4	83.280 ± 4.097	2.5	390.54 ± 17.29
4.2	0.9463	0.0053 ± 0.0011	0.117 ± 0.040	0.048 ± 0.011	87.518 ± 3.423	1.8	85.937 ± 3.370	1.9	401.71 ± 14.13
5	0.1081	0.0286 ± 0.0135	0.704 ± 0.384	0.039 ± 0.017	81.498 ± 2.748	10.4	73.005 ± 4.389	0.2	346.69 ± 18.96
6	0.9462	0.0052 ± 0.0010	0.093 ± 0.035	0.054 ± 0.011	89.249 ± 1.639	1.7	87.713 ± 1.625	1.9	409.14 ± 6.78
12	2.7315	0.0014 ± 0.0004	0.027 ± 0.021	0.058 ± 0.011	94.815 ± 1.158	0.4	94.399 ± 1.155	5.5	436.83 ± 4.75

* P, power; as measured by laser in % of full nominal power (10 W). † Fraction ^{39}Ar as percent of total run. §Errors are analytical only and do not reflect error in irradiation parameter J. # Nominal J, referenced to FCT-SAN = 28.02 Ma (Renne *et al*. 1998). Note: All uncertainties quoted at 2σ level. *^{40}Ar, radiogenic ^{40}Ar.

https://doi.org/10.1017/S001675680400041X Published online by Cambridge University Press